

Plasma Filamentation in the Rijnhuizen Tokamak RTP

N. J. Lopes Cardozo, F. C. Schüller, C. J. Barth, C. C. Chu, F. J. Pijper, J. Lok, and A. A. M. Oomens
FOM-Instituut voor Plasmafysica "Rijnhuizen," P.O. Box 1207, 3430 BE Nieuwegein, The Netherlands
 (Received 17 February 1994)

Evidence for small scale magnetic structures in the Rijnhuizen tokamak RTP is presented. These are manifest through steps and peaks in the electron temperature and pressure, measured with multiposition Thomson scattering. During central electron cyclotron heating, several filaments of high pressure are found in the power deposition region. They live hundreds of microseconds. Near the sawtooth inversion radius a "step" in the temperature profile occurs. Further out, quasiperiodic structures are observed, in both Ohmic and heated discharges.

PACS numbers: 52.35.-g, 52.50.Gj, 52.55.-s

A tokamak plasma is usually considered as a medium in which particle density, temperature, and current density are smooth functions of the minor radius of the torus. The helical magnetic field lines are assumed to lie on closed toroidal flux surfaces which form a nested set. It is well known that this picture is an idealization. Flux surfaces on which the normalized pitch of the field lines (q) is a rational number can degenerate to form magnetic islands. These can be detected experimentally if they reach macroscopic dimensions, as is the case in, e.g., precursors and postcursors of the sawtooth instability and prior to disruptions.

Apart from these macroscopic magnetohydrodynamic (MHD) instabilities, small scale magnetic structures are normally not observed, possibly because their dimensions are so small that they escape detection. This may be the reason why in most transport theories the idealized magnetic structure is assumed. However, even small magnetic structures can have a strong impact on the transport of heat and particles (see, e.g., [1-3]).

Experimental evidence for the existence of such structures is scarce (e.g., [4-7]) or applies to the cool edge of the plasma [8,9]. In JET [7], flat regions were observed in the electron temperature profile, which were interpreted as evidence for the existence of a helical mode structure. In TFTR, however, in a dedicated search no structures in the electron cyclotron emission could be found [10], which was interpreted as the absence of electron temperature structures. In this paper we present measurements from the Rijnhuizen Tokamak Project (RTP) that are of a similar nature to those in JET, but show much more pronounced features. Essential differences with respect to the JET work are a better measuring resolution and a higher power density for additional heating ($\approx 10 \text{ MW/m}^3$).

RTP (major/minor radius 0.72 m/0.165 m, toroidal field 2.2 T, boronized vessel) is equipped with electron cyclotron heating (ECH) (60 GHz waves launched in O mode from the low field side or in X mode from the high field side, or both; nominal power $2 \times 180 \text{ kW}$, pulse duration $< 100 \text{ ms}$ [11]) and an extensive set of diagnostics, including magnetics, 19-channel far-infrared interferometer, 20-channel heterodyne radiometer, 80-

channel 5-camera soft x-ray tomographic system, etc. Crucial for the present study is the Thomson scattering system, which measures the electron temperature (T_e) and density (n_e) along a vertical chord through the center of the plasma at 100 radial positions simultaneously, with a spatial resolution of 1.7 mm [12]. In this Letter, we report measurements of small scale structures in the T_e profile under conditions of strong central heating, measured with this diagnostic. Indications for the existence of such structures were already obtained previously [5].

The light source of the multiposition Thomson scattering diagnostic is a single pulse ruby laser (Lumonics, $\lambda_0 = 694.3 \text{ nm}$, 25 J in a 15 ns pulse). Scattered light is imaged on the slit of a Litrow polychromator. The light of the resolved spectrum is amplified by a gated image intensifier, with a GaAs photocathode. The amplified image is detected with a cooled charge coupled device, of which the pixels are grouped such that the radial resolution $\Delta r = 1.7 \text{ mm}$ and the spectral resolution $\Delta \lambda = 3.6 \text{ nm}$ match the slit width. In a single laser pulse 100 spectra are obtained along the viewing chord. The spectra are resolved into 64 wavelength channels, covering the range 580 to 800 nm. The system is calibrated *in situ* with a tungsten ribbon lamp. T_e and n_e are determined by a weighted three-parameter fit of the theoretical (relativistic) curve to the measured spectrum [13]. Figure 1(a) shows a measured spectrum and the fitted curve. To bring out the overall performance of the system, in Fig. 1(b) the photon noise has been reduced by adding 20 spectra of approximately equal T_e . Except for the central laser line and the H_α line, which have been cut from the spectrum, systematic distortions of the spectrum are small. Plasma light (except H_α) is normally below the detection threshold, thanks to the high brightness of the laser and the short (100 ns) gate pulse of the detector.

In individual spectra photoelectron statistics cause significant scatter of the measured spectral intensities. An error analysis was carried out by simulating spectra including the photoelectron statistics. Thus an estimate of the random error on T_e , σ_T , as a function of T_e was obtained. An independent estimate was obtained using measured spectra, for which σ_T was computed from the least

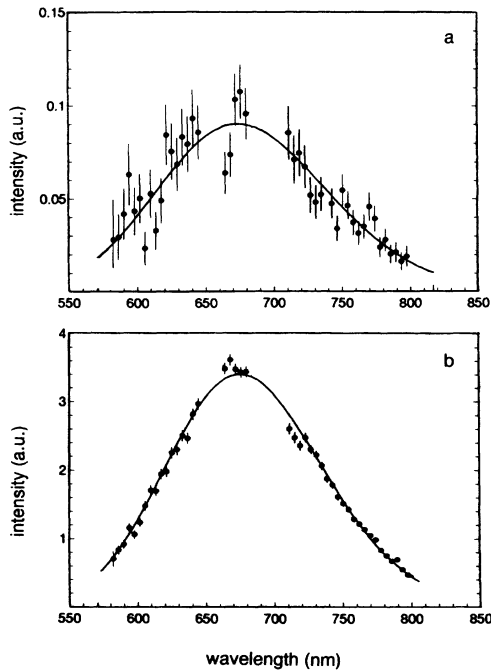


FIG. 1. (a) A measured Thomson scattering spectrum and the fitted theoretical curve ($T_e = 2.0$ keV, $n_e = 2.5 \times 10^{19} \text{ m}^{-3}$) (b) Average of 20 spectra with $T_e \approx 1.7$ keV, showing that systematic distortions are small.

squares fit of the theoretical curve to the data. The two independent estimates of σ_T were in good agreement (see Fig. 2). In the remainder of this paper, the error estimation of the fitting procedure is used.

T_e and n_e profiles were measured in Ohmic and ECH heated hydrogen plasmas, for a variety of plasma parameters: edge safety factor $q_a = 3.2-16$; line averaged density $\bar{n}_e = (1-2) \times 10^{19} \text{ m}^{-3}$. Typically, the global energy confinement time is $\tau_E \approx 1-5$ ms. In ECH heated discharges, and ECH pulse (central deposition) of

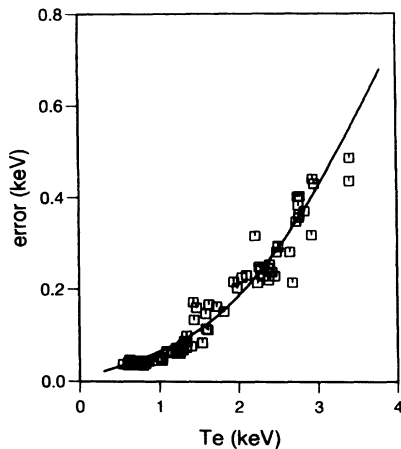


FIG. 2. Two independent estimators of the statistical error on T_e . Solid line: computer simulation, assuming photon statistics to be the dominant error component. Boxes: error estimation of the least squares fit to experimental data.

>50 ms was applied in the current flattop. The Thomson scattering measurement was carried out 5 ms before the end of the ECH pulse. During the ECH pulse, no MHD activity is observed on the Mirnov coils.

The measured T_e profiles show distinct features. Typical observations are the following: (i) hot filaments in the plasma core (Fig. 3), (ii) steps of T_e , apparently associated with the sawtooth inversion radius (Fig. 4), and

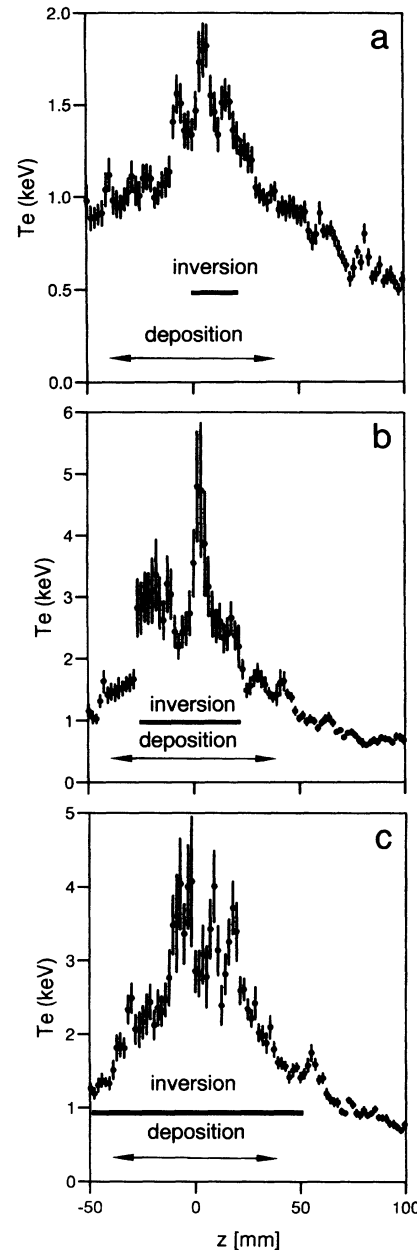


FIG. 3. Examples of T_e profiles during the ECH pulse showing distinct filamentation in the central plasma. (a) $q_a = 10$; (b) $q_a = 5.1$; (c) $q_a = 3.2$. The limiter is at $z = 165$ mm. Single pass absorption of ECH puts >100 kW within $r \approx 3.5$ cm (indicated by “deposition”). The sawtooth inversion radius determined by ECE. When this method fails (at $q_a > 6$ the scaling $r_{inv} = a/q_a$ is used.

(iii) quasiperiodic structures outside the sawtooth region. The profiles of n_e are rather flat, and, if there are structures to be discerned, their relative excursions are an order of magnitude smaller than those on T_e . In other words, the electron pressure profile exhibits the same features as the T_e profile.

These observations challenge the standard model of the magnetic topology in a tokamak. We first consider the steps in T_e . These appear symmetrically on both sides of the axis. Their position is reproducible, scales

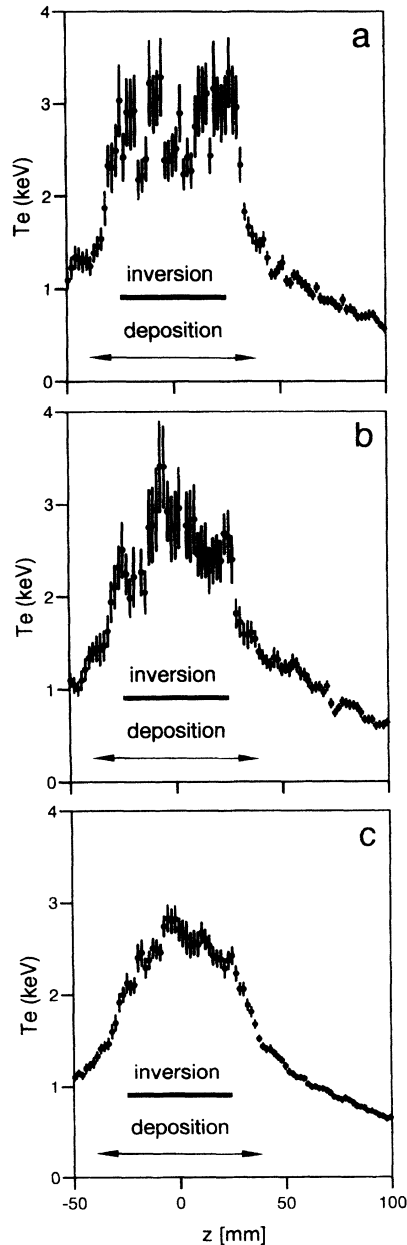


FIG. 4. Examples of T_e profiles showing strong gradients near the sawtooth inversion radius ($q_a = 6.7$). Case (c) is an averaged profile of 15 discharges with identical conditions. See caption of Fig. 3 for definitions of inversion and deposition.

with the plasma current, and is just outside the sawtooth inversion radius as determined with the electron cyclotron emission system. The steps are most pronounced at high q_a , where temperature gradients of up to 1 MeV/m have been observed at a density of $n_e \approx 2 \times 10^{19} \text{ m}^{-3}$. First, a sheet of high diamagnetic current density is directly implied by the strong pressure gradient. Also to satisfy the $\nabla p = \mathbf{j} \times \mathbf{B}$ equilibrium condition, a thin layer of large current density is required. Second, the abrupt change of ∇T_e implies a drop of the electron thermal diffusivity χ_e by up to 2 orders of magnitude over a distance of 2 mm. Both observations are of great significance for studies of transport in tokamaks. Moreover, the fact that such large pressure gradients may develop near the sawtooth inversion radius is a new and possibly important input to the theory of the sawtooth instability.

In the central region in many cases multiple peaks are observed in T_e . The area in which the high peaks occur appears to be limited to the region of high ECH power density, which in low q_a discharges is much smaller than the sawtooth region [Fig. 3(c)]. On the other hand, in high q_a discharges, the peaks were also found [Fig. 3(a)]. In this case it is unclear whether there is $q = 1$ surface at all: Sawteeth are not observed but may be too small for detection. Using the scaling $r(q = 1) \approx a/q_a$ a finite inversion radius is found, which is indicated in the figure.

The observation of multiple high T_e and high pressure regions in the plasma center is difficult to reconcile with the existence of nested flux surfaces. A working hypothesis is that the hot regions are closed flux tubes. The diffusivity inside the tubes must be very low to allow the high T_e values. An estimation obtained by assuming that a tube absorbs a fraction of the ECH power proportional to its surface relative to the deposition region gives $\chi_e(\text{inside}) \approx 0.01 \text{ m}^2/\text{s}$ for 6 mm diameter. This is 1 to 2 orders of magnitude lower than the diffusivity in the ambient plasma, approaching the neoclassical limit. Again, to maintain the pressure balance, it is necessary that there is a strong, "locally poloidal" current density inside the tube.

An experiment in which T_e was measured just after switching off the ECH power showed that the hot peaks have a lifetime of hundreds of μs (Fig. 5). This is in agreement with the low value of $\chi_e(\text{inside})$. It is important that this measurement shows that the magnetic structures are quite long lived: at least hundreds of μs .

Finally, the structures outside the sawtooth region, which are also observed in Ohmic discharges, will be the subject of a forthcoming publication: For a proper investigation a statistical analysis is required for which the present database is insufficient. However, there may be a relation to the (remnants of) rational q surfaces, similar to the structures invoked by Dubois *et al.* [6] to explain striations in the ablation cloud of a pellet injected into the plasma. It is also noted that the transport models by Rebut *et al.* [2] and by Kadomtsev [1] invoke "chains of

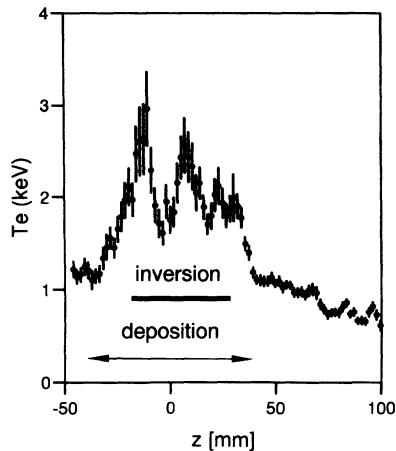


FIG. 5. T_e profile 300 μ s after switching off ECH, showing the persistence of the hot filaments ($q_a = 6.7$).

islands" at rational q surfaces, and similarly Hegna and Callen [14] predict flat spots in the T_e profile.

The question why no structures were found in the TFTR experiments may be partially answered by the following: (i) In RTP, the most pronounced features are observed in the central part of the discharge, where the power density and therefore the heat flux is extremely large, amplifying the variations in T_e gradients. (ii) Outside the sawtooth region, the features observed in RTP are less pronounced. Similar structures (scaled up) would go unnoticed in the TFTR setup.

In conclusion, we have presented evidence for the existence of small scale magnetic structures in a tokamak plasma. These include several closed flux tubes in the center of the discharge, a very steep pressure gradient and associated a strong diamagnetic current sheet near the sawtooth inversion radius, as well as structures in the confinement region. Inside the closed tubes and across the current sheet the thermal diffusivity is extremely low, close to neoclassical.

Discussions with D.C. Schram, an early protagonist of the "filamentation" concept, and colleagues at Rijnhuizen are gratefully acknowledged. We also thank the technical

staff of RTP who operated the tokamak and ECH equipment with great dedication. This work was performed under the Euratom-FOM association agreement, with financial support from NWO and Euratom.

-
- [1] B. B. Kadomtsev, Nucl. Fusion **31**, 1301 (1991).
 - [2] P. H. Rebut, M. Brusati, M. Hugon, and P. P. Lallia, in *Proceedings of the 11th International Conference on Plasma Physics and Controlled Nuclear Fusion Research, Kyoto, 1986* (IAEA, Vienna, 1987), Vol. 2, p. 187.
 - [3] J. B. Taylor, Phys. Fluids B **5**, 4378–4383 (1993).
 - [4] P. Cripwell and A. E. Costley, in *Proceedings of the 18th EPS Conference on Controlled Fusion and Plasma Physics, Berlin, 1991* (European Physical Society, Petit-Lancy, 1991), Pt. 1, p. 17.
 - [5] N. J. Lopes Cardozo and F. C. Schüller, Plasma Phys. Controlled Fusion **34**, 1939–1944 (1992).
 - [6] M. A. Dubois, B. Pégourié, R. Sabot, and G. T. Hoang, in *Proceedings of the 1992 International Conference on Plasma Physics, Innsbruck, 1992* (European Physical Society, Petit-Lancy, 1992), Pt. I, p. 103.
 - [7] M. F. F. Nave, A. W. Edwards, K. Hirsch, M. Hugon, A. Jacchia, E. Lazzaro, H. Salzmänn, and P. Smeulders, Nucl. Fusion **32**, 825–835 (1992).
 - [8] S. J. Zweben and S. S. Medley, Phys. Fluids B **1**, 2058 (1989).
 - [9] M. Malacarne and P. A. Duperrex, Nucl. Fusion **27**, 2113 (1987).
 - [10] M. C. Zarnstorff *et al.*, in *Proceedings of the Workshop on Local Transport Studies in Fusion Plasmas, Varenna, 1993* (Editrice Compositori, Bologna, 1994), p. 257.
 - [11] F. C. Schüller *et al.*, in *Proceedings of the 14th International Conference on Plasma Physics and Controlled Nuclear Fusion Research, 1992, Würzburg, 1992* (IAEA, Vienna, 1993), Vol. 1, pp. 609–615.
 - [12] C. J. Barth, M. L. P. Dirx, B. J. J. Grobden, G. C. H. M. Verhaag, A. T. M. Wilbers, and A. J. H. Donné, Rev. Sci. Instrum. **63**, 4947–4949 (1992).
 - [13] M. Mattioli, Report No. EUR-CEA-FC-752, 1974 (unpublished).
 - [14] C. C. Hegna and J. D. Callen, Phys. Fluids B **5**, 1804 (1993).